

Effects of growth temperature on the photovoltaic properties of RF sputtered undoped NiO thin films

M.S Jamal^{a,b}, S.A. Shahahmadi^c, P. Chelvanathan^a, Hamad F. Alharbi^d, Mohammad R. Karim^e, Mushtaq Ahmad Dar^e, Monis Luqman^d, Nabeel H. Alharthi^d, Yahya S. Al-Harathi^f, M. Aminuzzaman^g, Nilofar Asim^a, K. Sopian^a, S.K. Tiong^c, Nowshad Amin^{c,h}, Md. Akhtaruzzaman^{a,h,*}

^a Solar Energy Research Institute, Universiti Kebangsaan Malaysia, 43600 Bangi, Selangor, Malaysia

^b Institute of Fuel Research and Development, BCSIR, Dhaka 1205, Bangladesh

^c Institute of Sustainable Energy, Universiti Tenaga Nasional (@The National Energy University), Jalan IKRAM-UNITEN, 43000 Kajang, Selangor, Malaysia

^d Mechanical Engineering Department, King Saud University, P.O. Box 800, Riyadh 11421, Saudi Arabia

^e Center of Excellence for Research in Engineering Materials, King Saud University, Riyadh 11421, Saudi Arabia

^f Electrical Engineering Department, King Saud University, P.O. Box 800, Riyadh 11421, Saudi Arabia

^g Department of Chemical Science, Faculty of Science, Universiti Tunku Abdul Rahman, Perak Campus, Jalan Universiti, Bandar Barat 31900, Kamapar, Perak D. R., Malaysia

^h INTEGRA, FKAB, Universiti Kebangsaan Malaysia, 43600 Bangi, Selangor, Malaysia

ARTICLE INFO

Keywords:

Magnetron sputtering
Material properties NiO thin film
Substrate temperature
Transparent conducting oxide

ABSTRACT

In this study, nickel oxide (NiO) thin films were deposited on soda lime glass using radio-frequency magnetron sputtering at different growth (substrate) temperatures ranging from room temperature (RT) to 400 °C. The effects of substrate temperature on the structural, morphological, electrical, and optical properties were investigated. The XRD pattern unveiled a dominant peak with (2 0 0) preferential orientations for the film grown at 100 °C. However, for samples grown at high temperatures, a gradual decrease of (2 0 0) peak intensity was observed, which may be the result of the decomposition of NiO as confirmed via EDX. Surface morphology from FESEM revealed that grains were randomly orientated on the surface with maximum grain size of 19.43 nm. Upon increasing the growth temperature, the crystal quality and grain size substantially deteriorated, which is consistent with the XRD results. Scanning probe microscopy (SPM) finds rough surface with the highest surface roughness obtained at RT with a value of 1.232 nm. Electrical resistivity was found to be highly dependent on the growth temperature that decreases from 2150 Ω cm to 72 Ω cm as the substrate temperature increases. For optical properties, the optical bandgap of the NiO films decreases from 3.8 eV to 3.2 eV as a function of substrate temperature as derived from the optical transmittance data. Results show the potential application of the NiO films in photovoltaic devices.

Introduction

Nickel oxide (NiO) is a semi-transparent and naturally p-type semiconductor, which has a wide bandgap ranging from 3.6 eV to 4.0 eV. Recently, NiO has drawn tremendous attention owing to its exceptional optical, electrical, and magnetic properties and good chemical stability. The remarkable inherent properties of NiO has enabled this compound to become a promising material for photovoltaic solar cells [1], electrochromic devices [2], ultraviolet photo-detectors [3], and gas sensors [4]. In solar cells, two main applications are anticipated

for NiO: either as a transparent conducting oxide (TCO) [5] or hole transporting layer (HTL) in perovskite solar cells [6,7]. In particular, replacing organic HTL to inorganic is important because the latter has high hole mobility, easily processable properties, low production cost, and highly stable [8]. Deposition temperature is another crucial issue to grow any layer on the top of the perovskite absorber because it easily decomposes when exposed at > 150 °C, although the precise value is disputable [9]. Several physical and chemical methods have been used to fabricate NiO film, including spray pyrolysis [10], radio frequency (RF) magnetron sputtering [11,12], direct-current (DC) magnetron

* Corresponding author at: Solar Energy Research Institute, Universiti Kebangsaan Malaysia, 43600 Bangi, Selangor, Malaysia.

E-mail address: akhtar@ukm.edu.my (Md. Akhtaruzzaman).

<https://doi.org/10.1016/j.rinp.2019.102360>

Received 8 March 2019; Received in revised form 16 May 2019; Accepted 16 May 2019

Available online 24 May 2019

2211-3797/© 2019 The Authors. Published by Elsevier B.V. This is an open access article under the CC BY license

(<http://creativecommons.org/licenses/by/4.0/>).

sputtering [13], chemical bath deposition [14], chemical vapor deposition [15], electron beam evaporation [16], sol-gel method [17], and pulsed laser deposition [18]. Among these methods, RF magnetron sputtering is the most widely used for the deposition of the NiO thin film. The main advantages of RF sputtering are uniform thickness, pinhole free thin film, and deposition over a large surface area owing to the high kinetic energy of the sputtered atoms on the substrate holder. In this method, the properties of thin films are mainly defined by RF power, substrate temperature, sputtering pressure, target-substrate distance, and system geometry [19–22].

Ahmed et al. [11] demonstrated that the structural quality of NiO deteriorated upon increasing the substrate temperature to over 100 °C because of the possible decomposition of NiO. Sato et al. [5] showed the effect of sputtering pressure and RF power on the resistivity and transmittance of NiO thin film. Chen et al. [23] reported that the deposition rate, resistivity, and surface roughness of NiO thin film decreased as substrate temperature increased, whereas the transmittance of NiO film increased with substrate temperature. Ai et al. [12] investigated the effect of substrate temperature on the resistivity and optical bandgap of NiO thin film. Their findings indicated that the resistivity and optical bandgap of NiO films increased with substrate temperature. The majority of previous studies have focused on the deposition of NiO through RF magnetron sputtering using the Ni target in the presence of O₂. However, the growth of NiO thin film by using NiO compound in single target by RF magnetron sputtering has rarely been reported. The ultimate focus of the present study is to deposit a compact and homogeneous NiO thin film via RF magnetron sputtering to investigate its application as HTL in perovskite solar cells. An ideal HTM should fulfill some general requirements to work efficiently in perovskite solar cells. High optical transmittances, sufficient hole mobility, matching energy level, and excellent thermal and photochemical stability are the essential requirements to achieve good photovoltaics properties. Transmittance of light through HTM should be as high as possible to avoid wasting photon energy in HTM before being absorbed by the perovskite layer. High hole mobility is essential for effective hole transporting to the anode and cathode for the p-i-n and n-i-p perovskite solar cells, respectively. Lastly, HTM should not react with the adjacent layer of perovskite solar cell. Hence, this explored the effects of substrate temperature on the structural, optical, and electrical properties along with surface morphology of un-doped NiO thin films deposited via RF magnetron sputtering from a stoichiometric NiO single target.

Experimental procedure

NiO thin films were deposited via RF magnetron sputtering onto well-cleaned soda lime glass (SLG) substrates (30 mm × 30 mm × 1.1 mm) at room temperature. Substrates were cleaned ultrasonically in soap water–deionized water–methanol–isopropanol–deionized water sequence. Thereafter, the substrates were dried in N₂ gas flow and rinsed in acetone. Lastly, substrates were exposed under UV for 30 min to remove organic residues. Stoichiometric NiO sputtering target (diameter: 2 in; purity 99.99%, custom-made) was used as the source material. The diameter and thickness of the NiO sputtering target were 50 mm and 5 mm, respectively. The distance between target and substrate was maintained at 14 cm. Prior to sputtering, the target was pre-sputtered for 15 min at 50 W power to clean the target surface. The base pressure, working pressure, sputtering power, and deposition time were maintained at 5×10^{-6} Torr, 28 m Torr, 50 W, and 90 min, respectively. The reactive gas was high-purity Ar (99.9999%) and the flow rate was 4 sccm as controlled by a mass flow controller. The rotation speed of the substrate holder was maintained at 10 rpm during sputtering. Prior to sputtering, the substrates were preheated for 45 min at intended deposition temperature of 100–400 °C.

BRUKER aXS-D8 Advance Cu-K α diffractometer was used to measure the structural and crystallographic properties of NiO thin films. X-

ray diffraction (XRD) patterns were recorded in the diffraction angle (2 θ) ranging from 20° to 70° using Cu K α radiation wavelength, $\lambda = 1.5406$ Å. NT-MDT, NTEGRA PRIMA scanning probe microscopy (SPM) in noncontact mode setting was used to investigate the surface topography and roughness of the NiO thin film. Optical transmission and absorbance measurements were performed using Perkin Elmer Lambda 950 UV/Vis/NIR spectrophotometer in the wavelength range of 200–1000 nm. The Hall Effect Measurement system called HMS ECOPIA 3000 (magnetic field 0.57 T, probe current 10 mA) was used to measure the electrical parameters, including carrier concentration, mobility, and resistivity. Lastly, SUPRA 55 VP field emission scanning electron microscope (FESEM) was used to measure the film thickness, grain size, surface morphologies, and cross-sectional view with accelerating voltage of 10–20 kV, which is equipped with energy dispersive x-ray (EDX) detectors.

Results and discussion

Structural analysis of the NiO films

The XRD pattern of the NiO thin films with diffraction angles from 20° to 70° at different substrate temperatures is shown in Fig. 1(a). The diffraction patterns of the RF-sputtered NiO films show that all samples exhibit two diffraction peaks corresponding to NiO (2 0 0) and Ni (2 2 0) orientations at 43.3° and 62.5°, respectively, except the sample sputtered at 400 °C. The XRD pattern from this study is appropriately matched with the standard XRD spectrum documented in JCPDS card No. 00-047-1049, thereby representing that the grown polycrystalline NiO layer crystallizes in a cubic structure. The dominant peak intensity

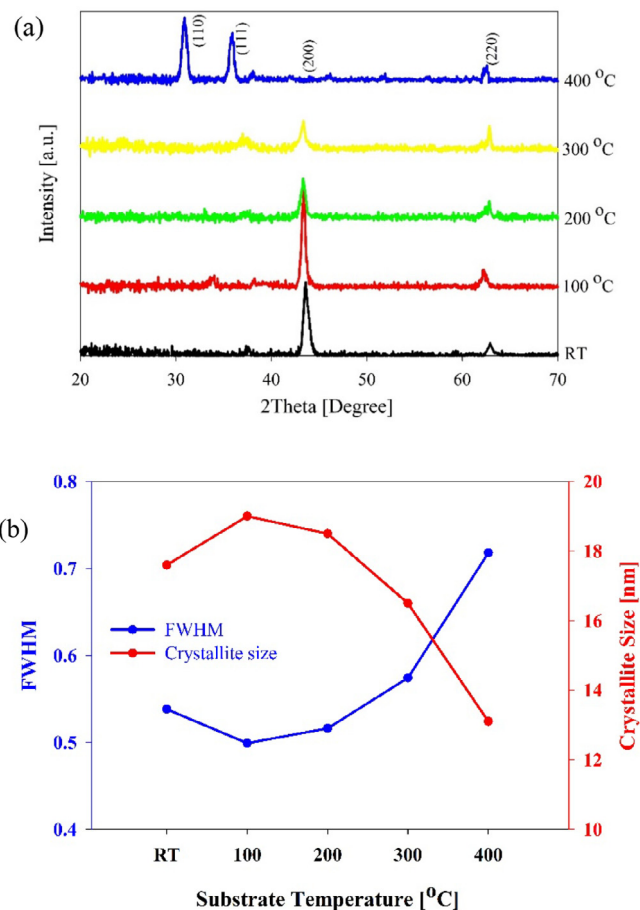


Fig. 1. Structural properties of the NiO thin films at different substrate temperatures, (a) XRD pattern, (b) variations of FWHM, and crystallite size.

is seen at substrate temperature 100 °C, thereby indicating strong orientation and good crystallinity. The (2 0 0) intensity of NiO diffraction peak steadily decreases as substrate temperature continues to increase. At 400 °C, the crystal quality of NiO films are entirely degraded and diffraction peaks along (1 1 1) and (1 1 0) planes appeared at 35.89° and 30.92°, respectively. At substrate temperature of over 100 °C, the crystallinity of NiO films is degraded by the high thermal energy available to the adatoms of NiO films. This result may be ascribed to low atomic mobility at low substrate temperature, thereby leading to the formation of a preferred orientation along the (2 0 0) plane. However, when the substrate temperature increased, the NiO atoms gain additional energy and tend to move another preferred orientation along the (1 1 1) and (1 1 0) planes. This experiment was conducted via RF sputtering of the NiO target. Thus, NiO is partially dissociated into metallic Ni and O at high substrate temperature. This phenomenon leads to a reduction of the crystal quality of NiO thin films. These observations are in good agreement with prior studies that reported a decrease in the crystallinity of different thin films owing to their decomposition at high substrate temperatures [11,24]. Several structural parameters, including crystallite size, FWHM, strain, dislocation density, microstrain, and lattice parameter, were calculated from the XRD data. Fig. 1(b) represents the variations of crystallite size and FWHM of the NiO diffraction peaks along the (2 0 0) plane corresponding to different substrate temperatures. The average crystallite size (d_{hkl}) was estimated using the Debye-Scherrer's equation [25]:

$$d_{hkl} = k\lambda/(\beta\cos(2\theta)) \quad (1)$$

where λ is the X-ray wavelength, β is the FWHM intensity of the main peak observed at 2θ in radian, θ is the Bragg's angle of diffraction, and k is a constant. Fig. 1(b) shows that the crystallite size of NiO decreases with increasing substrate temperature, although FWHM increases. The crystallite size decreased from 19.43 nm to 13.10 nm as the substrate temperature increased from RT to 400 °C. This result is ascribed to the low surface diffusion of the adatoms on the substrate because of the decomposition of the NiO thin film at high substrate temperature [11]. The microstrain (ϵ) and dislocation density (δ) of the NiO thin films were calculated using Eqs. (2) and (3), respectively [26,27]:

$$\epsilon = \beta/(4\tan\theta) \quad (2)$$

$$\delta = n/D^2 \quad (3)$$

where D is the grain size and n is a factor that is nearly equal to the unity for minimum dislocation density.

Fig. 2(a) depicts the variations of the calculated dislocation densities and microstrain for the (2 0 0) crystallographic orientation of the NiO films sputtered at different substrate temperatures. The increasing degree of microstrain and dislocation density is found for films sputtered at high substrate temperatures. Grain size enlargement through grain fusion at high substrate temperature reduces the lattice point mismatch of two adjacent crystals. Lattice point mismatch initiates from the misregistry of the lattice in one part of the crystallite with respect to another part along the interconnecting grain boundary. Fig. 2(a) shows decreased dislocation density and microstrain at low substrate temperature caused by low lattice point mismatch that eventually becomes favorable for photovoltaic application. The collective impact of the increase in the microstrain and dislocation density can be used to clarify the substantial enhancement in the stacking fault of films with increasing substrate temperature [28].

The variation of the lattice constant and percentages of change in the lattice constant (strain) along the plane (2 0 0) crystallographic orientation as a function of substrate temperature are presented in Fig. 2(b). The lattice constant of the NiO thin films was calculated using Eq. (4) [29]:

$$\frac{1}{d_{hkl}^2} = (h^2 + k^2 + l^2) \frac{1}{a^2} \quad (4)$$

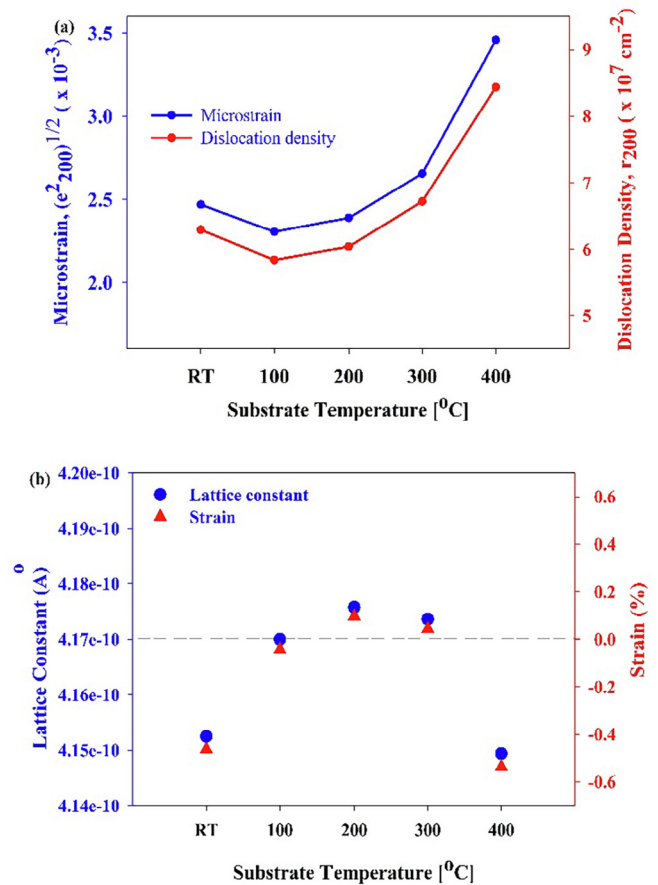


Fig. 2. (a) Effect of growth temperature on microstrain and dislocation density (b) lattice constant and strain of the NiO thin film.

The dotted line in the graph indicates the equilibrium lattice constant value, which corresponds to 0% strain. The lattice constant and strain of the NiO film increased with substrate temperature. Growing substrate temperature encourages lattice relaxation with film sputtered at 100 °C maintaining equilibrium lattice parameter without strain. Fig. 2(b) reveals that the equilibrium lattice constant of the RF-sputtered NiO at 100 °C is 4.17 Å at zero strain. This result is consistent with the previous experimental finding of Madhavi et al. [17]. The variations in the lattice constant and strain with substrate temperature are due to the tensile stress developed in the films at high substrate temperature [30]. Consequently, the film will crack or shrink because of compressive strain, which could not be observed by the naked eye but is detrimental for photovoltaic application.

Surface morphology of the NiO films

The variation of surface morphology and the cross-sectional view of the NiO thin films at different substrate temperatures were observed via FESEM (see Fig. 3). The FESEM micrograph demonstrates the nano-scale grain of the NiO thin films and the grain size is strongly dependent on the substrate temperature. The FESEM micrograph of NiO deposited at 100 °C possess uniform grain size and high packing density with an average grain of ~16 nm. Grain size and crystal quality rapidly deteriorated with increasing substrate temperature. Interestingly, the grain shapes completely become irregular at 400 °C. This morphological observation is in good agreement with the previously discussed structural analysis of the NiO thin film. From the cross-sectional view, thickness gradually decreases as substrate temperature increases. Thickness is reduced from 100 nm to 60 nm as substrate temperature increased from RT to 100 °C. This outcome may be the result of the dependency

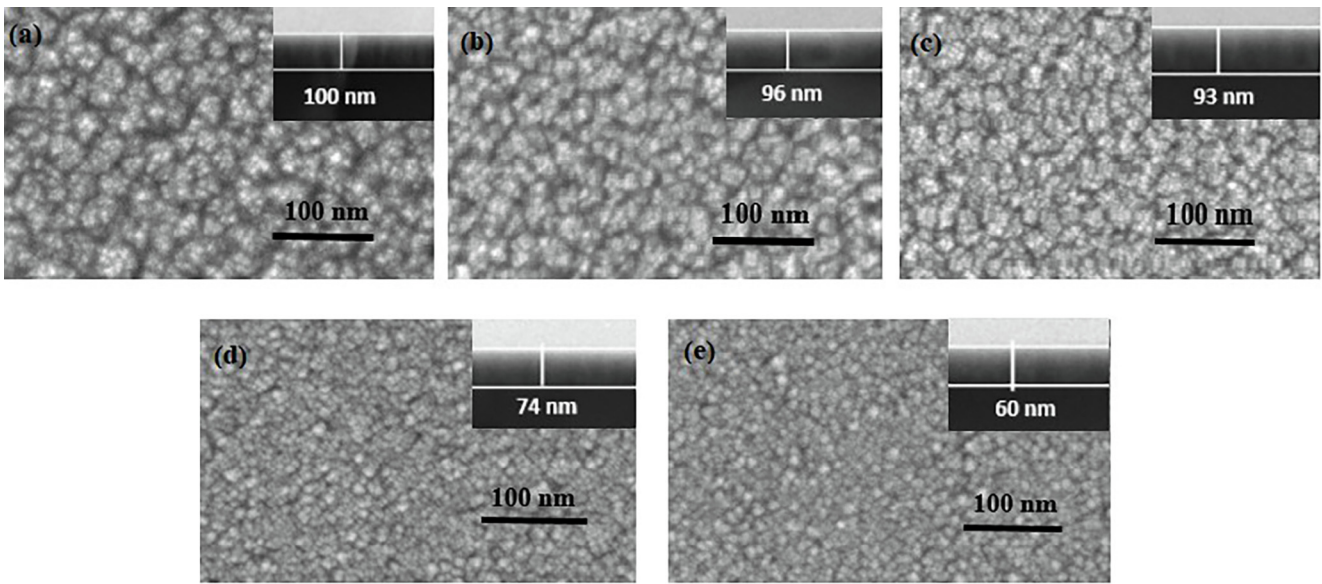


Fig. 3. Top and cross-sectional (inset) views of the NiO thin film at different substrate temperatures: (a) RT, (b) 100 °C, (c) 200 °C, (d) 300 °C, and (e) 400 °C.

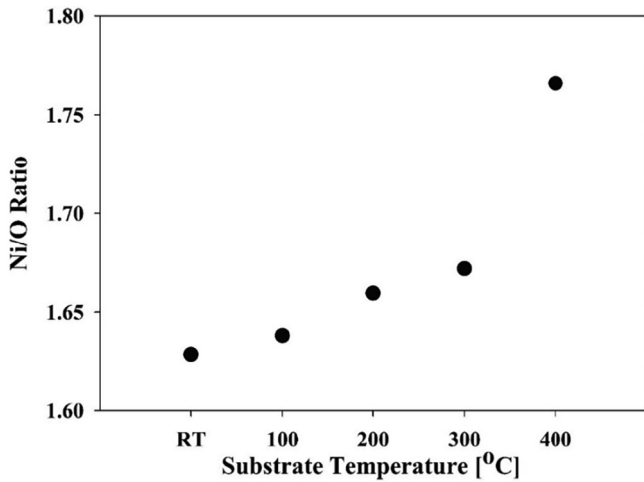


Fig. 4. Variation in the Ni/O ratio as a function of substrate temperature.

Table 1

Hall parameters of the NiO thin films at different substrate temperatures.

Substrate temperature, °C	Carrier concentration, cm ⁻³	Carrier mobility, cm ² /Vs	Resistivity, Ω cm
RT	6.08×10^{14}	6.73	1503
100	2.85×10^{14}	10.20	2150
200	4.49×10^{14}	6.75	2060
300	7.32×10^{15}	2.87	298
400	3.87×10^{16}	2.23	72

between grain size and film thickness [31]. The effect of Ni/O ratio on the substrate temperature is shown in Fig. 4. The ratio of Ni/O increased with substrate temperature because the NiO atoms decomposed at high substrate temperature, thereby leading to the degradation of crystal quality. This observation reveals a correlation among the structural properties of NiO thin film and is consistent with the findings of Ahmed et al. and Reddy et al. [11,32].

The surface roughness analysis of NiO thin films deposited at

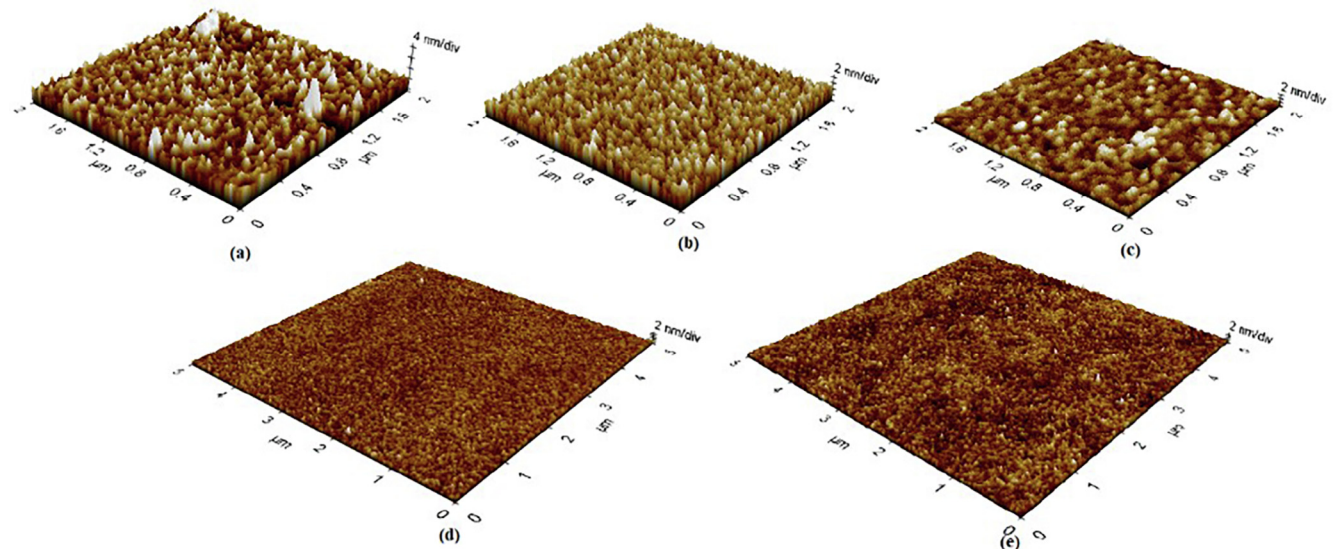


Fig. 5. 3D SPM images of the NiO thin films deposited by RF sputtering at different substrate temperatures: (a) RT, (b) 100 °C, (c) 200 °C, (d) 300 °C, and (e) 400 °C.

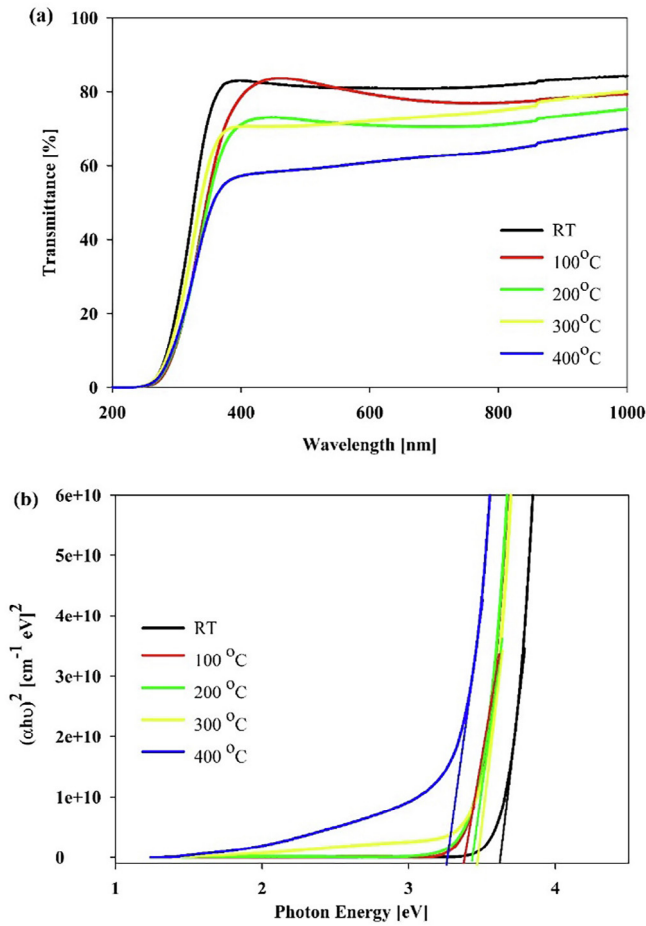


Fig. 6. (a) Spectral transmittance and (b) tauc plot of the NiO thin films deposited at different substrate temperatures.

different substrates (Si wafer) was carried out through SPM. The 3D SPM images of the NiO thin films are shown in Fig. 5. The average roughness of the substrate is defined as the proportion of the root means square (RMS) value to the average height. The values of the RMS surface roughness at substrate temperatures RT, 100 °C, 200 °C, 300 °C, and 400 °C are observed to be 1.232 nm, 1.046 nm, 0.681 nm, 0.632 nm, and 0.621 nm, respectively. Hence, surface roughness decreased as substrate temperature increased, thereby correlating with the structural analysis via XRD. The crystalline quality of the NiO thin films has been improved at low temperature. This property may help induce additional ordered packing of molecules to eliminate voids and dislocations and can act as charge traps. A similar experimental output is also reported by Fasaki et al. [31].

Electrical properties of the NiO films

Table 1 shows the electrical properties of the NiO thin films. The growth of these films at various substrate temperatures unveils a p-type conductivity with carrier concentration from $2.85 \times 10^{14} \text{ cm}^{-3}$ to $3.87 \times 10^{16} \text{ cm}^{-3}$, thereby reflecting the substantial influence of substrate temperature on the electrical properties of NiO. The variation of electrical conductivity of the NiO thin films at different substrate temperatures depends on the microstructural defects of the NiO crystal and surface chemical reaction [23]. The XRD studies indicate that the crystallinity structure decreases as the substrate temperature increases owing to microstructural defect, thereby increasing carrier concentration [33]. The relation among carrier concentration, carrier mobility, and resistivity can be explained by Eqs. (5) and (6):

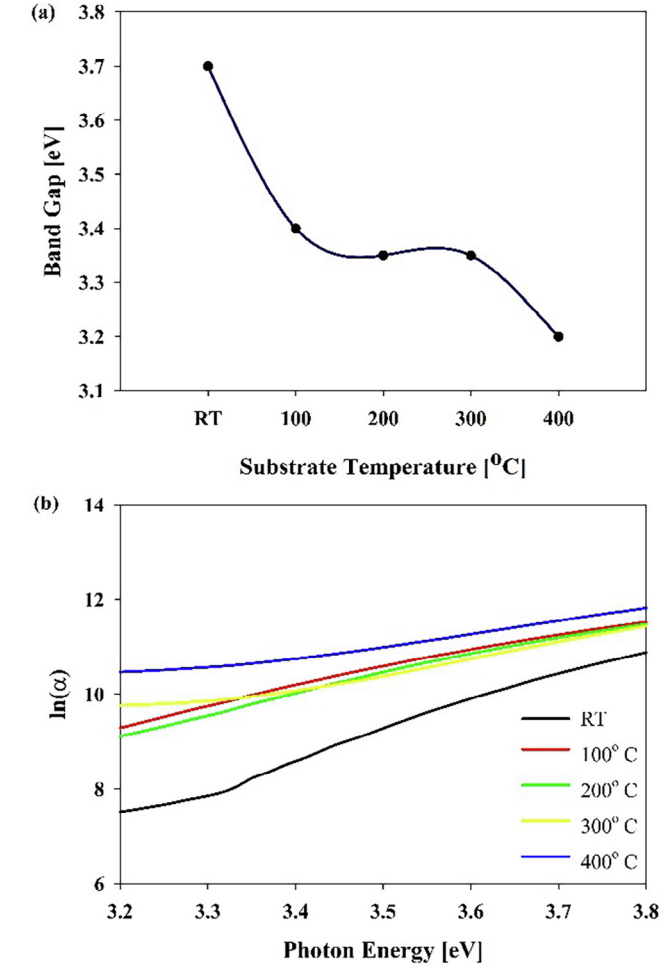


Fig. 7. (a) Band gap and (b) Urbach energy of the NiO thin films deposited at different substrate temperatures.

Table 2
Urbach energy of the NiO thin films at different substrate temperatures.

Substrate Temperature, °C	Urbach energy, meV
RT	177
100	264
200	250
300	354
400	438

$$\sigma = q\eta\mu_h \tag{5}$$

$$\sigma = \frac{1}{\rho} \tag{6}$$

where σ , ρ , q , η , and μ_e are conductivity, resistivity, electrical charge, carrier concentration, and carrier mobility, respectively. From the equations, electrical mobility and carrier concentration are inversely proportional to the resistivity. The carrier mobility of the NiO thin film initially increased with the substrate temperature along with decreasing resistivity. After 100 °C, the carrier mobility gradually decreased with continuous increasing substrate temperature and decreasing resistivity. This outcome could be caused by the increase in the dislocation density as presented in Fig. 2(a), which promotes carrier scattering and subsequently reduces carrier mobility. The NiO thin films showed a high electrical resistivity of 2150 Ω cm at a substrate temperature of 100 °C. The resistivity of the NiO thin films decreased to 72 Ω cm as substrate temperature increased to 400 °C because of increasing carrier

Table 3
Comparative studies of the experimental results of NiO with previous findings.

Target	Sputter-ing gas	Temp, °C	Power, Watt	Substrate	Thickness, nm	Transmittance, %	Band gap, eV	Crystal size, nm	Resistivity, ohm cm	Ref.
NiO	N ₂	RT–400	50	SLG	60–100	60.56–83.69	3.2–3.8	13.10–19.43	72 to 2150	This work
NiO	Ar	RT–300	200	Si	350–358	–	3.72–3.64	20.38–41.29	–	[11]
Ni	N ₂ /O ₂	RT–400	250	Fused Si	300	25–70	3.65–3.88	–	0.028–8.7	[12]
NiO	O ₂	RT–350	100–200	Corning Glass	–	60%	–	11.42–18.17	16.7	[23]

concentration, which is induced by Ni-rich composition through the partial decomposition of NiO at a high substrate temperature.

Optical characteristics of the NiO films

Substrate temperature strongly influences the optical transmittance of samples [24]. The optical transmittance of NiO was measured in the wavelength range of 200–1000 nm, as shown in Fig. 6(a). In the visible range, the transmittance of the NiO thin films decreases moderately as substrate temperature increases. The transmittance of these films is approximately 83.69% but drastically decreases thereafter to 60.56% as the substrate temperature increases from RT to 400 °C. These findings may be attributed to the increase in Ni content in NiO thin films, which coincidences with compositional analysis of this study. Pronounced light scattering is expected because of the large amount of grain boundaries and point defects that reflect the incident light [34].

The optical bandgap (E_g) of the NiO thin films at different substrate temperatures was calculated from the transmission spectra using the following equation [35]:

$$(\alpha h\nu)^2 = A(h\nu - E_g) \quad (7)$$

where α is the absorption coefficient, h is Planck's constant, ν is the incident photon frequency, A is the constant, and E_g is the optical bandgap. Fig. 6(b) shows the calculated E_g at different substrate temperatures and shows the values ranging from 3.80 eV to 3.20 eV for changing the substrate temperature from RT to 400 °C, which is fitting in the range of standard reported value. E_g narrows as substrate temperature increases as presented in Fig. 7(a). The change in E_g is due to the change in the stoichiometry and crystallinity of the NiO thin films [36]. Moreover, E_g may change because of the shift in absorption edge and changing carrier concentration, which can be explained by the Burstein–Moss effect [32,37]. The Burstein–Moss effect indicates that the fermi level moves into the conduction band of a degenerated semiconductor that leads to energy band expansion [38]. Thus, the shrinkage effect is leading over the Burstein–Moss effect because E_g is reduced with the increasing substrate temperature.

The Urbach tail is the exponential region in the absorption spectrum, which is a function of the absorption coefficient and photon energy. It reveals the shifts between the tails of the conduction and valence bands. The Urbach tail appears in the poor-crystalline, disordered, and amorphous materials owing to the localized states of these materials, which are extending or narrowing the bandgap. Rahal et al. also reported that Urbach energy is closely related to the disorder in the film network [39]. In the low photon energy range, the Urbach empirical rule can be explained by the following equation [40]:

$$\alpha = \alpha_o \exp(h\nu/E_u) \quad (8)$$

where α is the absorption coefficient, $h\nu$ is the photon energy, α_o is a constant, and E_u represents the Urbach energy, which is dependent upon the temperature. The Urbach energy of the NiO thin films have been estimated from the slopes of $\ln(\alpha)$ versus photon energy ($h\nu$) plots (see Fig. 7(b)).

The inverted slope of $\ln(\alpha)$ versus photon energy ($h\nu$) plots determines the values of the Urbach energy (see Table 2).

The Urbach energy of the NiO films increases from 177 meV to 438 meV as substrate temperature increases from RT to 400 °C. The

highest Urbach energy is found at 400 °C, thereby indicating that the crystallinity becomes inferior and the degree of defect increases with temperature [41]. These defects and disorders may lead to the formation of delocalized state near the band level and the enhancement of the Urbach energy value. This finding offers appreciated information for the research community that the RF-sputtered NiO thin films deposited at low substrate temperature are beneficial for photovoltaic applications. The structural, optical, and electrical properties of the NiO thin films have been compared with previously reported findings (see Table 3).

Hence, the core scientific findings from this experimental study can be deduced as follows. The loss of O from the NiO thin film during high-temperature sputtering leads to Ni-rich composition, which ultimately reduces optical transmission (as well as the optical band gap) and electrical resistivity. Therefore, the careful selection of growth temperature is imperative to tailor the material properties of the NiO thin film according to their intended applications (e.g., TCO, HTL, buffer layer).

Conclusions

NiO thin films were deposited via RF magnetron sputtering at different substrate temperatures from RT to 400 °C on the top of a soda lime glass. Leading peak intensity was obtained at 100 °C and the crystal quality substantially deteriorated as the increase of substrate temperature over 100 °C. Surface roughness, film thickness, and crystallite size decreased as the substrate temperature increased. Microstrain and dislocation density were enhanced by the substrate temperature probably due to the released stress in the NiO thin film. The atomic percentage of Ni increased at high substrate temperature for a possible decomposition of O. The carrier concentration and carrier mobility of the NiO thin film increased, whereas resistivity decreased as the substrate temperature increased. The lowest resistivity obtained was 72 Ω cm at 400 °C. The optical properties revealed that the optical bandgap shrinks corresponding to the increase of Urbach energy at high substrate temperature. The results prove that the properties of the NiO thin film deposited at 100 °C are suitable for photovoltaic application, particularly as HTM of the perovskite solar cell.

Acknowledgement

This study was financially supported by the Fundamental Research Grant Scheme (Code: FRGS/1/2017/TK07/UKM/02/9) of the Ministry of Higher Education, Malaysia. The authors would also like to extend their appreciation to the Deanship of Scientific Research at King Saud University for funding this study through Research Group No. RGP-1438-025.

Appendix A. Supplementary material

Supplementary data to this article can be found online at <https://doi.org/10.1016/j.rinp.2019.102360>.

References

- [1] Islam MB, et al. NiOx hole transport layer for perovskite solar cells with improved stability and reproducibility. ACS Omega 2017;2(5):2291–9.

- [2] Pereira S, et al. Electrochromic behavior of NiO thin films deposited by e-beam evaporation at room temperature. *Solar Energy Mater. Solar Cells* 2014;120:109–15.
- [3] Hasan MR, et al. Self-powered p-NiO/n-ZnO heterojunction ultraviolet photo-detectors fabricated on plastic substrates. *APL Mater.* 2015;3(10).
- [4] Steinebach H, et al. H₂ gas sensor performance of NiO at high temperatures in gas mixtures. *Sens. Actuators B: Chem.* 2010;151(1):162–8.
- [5] Sato H, et al. Transparent conducting p-type NiO thin films prepared by magnetron sputtering. *Thin Solid Films* 1993;236(1–2):27–31.
- [6] Chowdhury TH, et al. Nanostructured NiOx as hole transport material for low temperature processed stable perovskite solar cells. *Mater. Lett.* 2018;223:109–11.
- [7] Wang K-C, et al. Low-temperature sputtered nickel oxide compact thin film as effective electron blocking layer for mesoscopic NiO/CH₃NH₃PbI₃ perovskite heterojunction solar cells. *ACS Appl. Mater. Interfaces* 2014;6(15):11851–8.
- [8] Rajeswari R, et al. Emerging of inorganic hole transporting materials for perovskite solar cells. *Chem. Record* 2017;17(7):681–99.
- [9] Yu X, Qin Y, Peng Q. Probe decomposition of methylammonium lead iodide perovskite in N₂ and O₂ by in situ infrared spectroscopy. *J. Phys. Chem. A* 2017;121(6):1169–74.
- [10] Reguig B, et al. Properties of NiO thin films deposited by intermittent spray pyrolysis process. *Appl. Surface Sci.* 2007;253(9):4330–4.
- [11] Ahmed AA, Devarajan M, Afzal N. Effects of substrate temperature on the degradation of RF sputtered NiO properties. *Mater. Sci. Semicond. Process.* 2017;63:137–41.
- [12] Ai L, et al. Influence of substrate temperature on electrical and optical properties of p-type semitransparent conductive nickel oxide thin films deposited by radio frequency sputtering. *Appl. Surface Sci.* 2008;254(8):2401–5.
- [13] Hotový I, et al. The influence of process parameters and annealing temperature on the physical properties of sputtered NiO thin films. *Vacuum* 2002;69(1–3):237–42.
- [14] Gomaa M, et al. Structural and optical properties of nickel oxide thin films prepared by chemical bath deposition and by spray pyrolysis techniques. *J. Mater. Sci.: Mater. Electron.* 2016;27(1):711–7.
- [15] Yeh W-C, Matsumura M. Chemical vapor deposition of nickel oxide films from bis- π -cyclopentadienyl-nickel. *Japanese J. Appl. Phys.* 1997;36(11R):6884.
- [16] Seike T, Nagai J. Electrochromism of 3d transition metal oxides. *Solar Energy Mater.* 1991;22(2–3):107–17.
- [17] Abdullah, M., et al. Preparation of nickel oxide thin films at different annealing temperature by sol-gel spin coating method, in: *AIP Conference Proceedings*, AIP Publishing, 2016.
- [18] Tanaka M, et al. Transition metal oxide films prepared by pulsed laser deposition for atomic beam detection. *Thin Solid Films* 1996;281:453–6.
- [19] Ferdaous M, et al. Compositional disparity in Cu₂ZnSnS₄ (CZTS) thin film deposited by RF-sputtering from a single quaternary compound target. *Mater. Lett.* 2018;221:201–5.
- [20] Ferdaous MT, et al. Interplay between variable direct current sputtering deposition process parameters and properties of ZnO: Ga thin films. *Thin Solid Films* 2018.
- [21] Shahahmadi S, et al. Properties of a-SiGe thin films on glass by Co-sputtering for photovoltaic absorber application. *J. Nanosci. Nanotechnol.* 2015;15(11):9275–80.
- [22] Shahahmadi S, et al. Ge-rich SiGe thin film deposition by co-sputtering in in-situ and ex-situ solid phase crystallization for photovoltaic applications. *Mater. Sci. Semicond. Process.* 2016;56:160–5.
- [23] Chen H-L, Lu Y-M, Hwang W-S. Characterization of sputtered NiO thin films. *Surface Coatings Technol.* 2005;198(1–3):138–42.
- [24] Jassim SA-J, Zumaila AARA, Al Waly GAA. Influence of substrate temperature on the structural, optical and electrical properties of CdS thin films deposited by thermal evaporation. *Results Phys.* 2013;3:173–8.
- [25] Patterson A. The Scherrer formula for X-ray particle size determination. *Phys. Rev.* 1939;56(10):978.
- [26] Williamson G, Hall W. X-ray line broadening from filed aluminium and wolfram. *Acta Metall.* 1953;1(1):22–31.
- [27] Williamson G, Smallman R. III. Dislocation densities in some annealed and cold-worked metals from measurements on the X-ray debye-scherrer spectrum. *Philos. Mag.* 1956;1(1):34–46.
- [28] Mahalingam T, et al. Microstructural characterization of electrosynthesized ZnTe thin films. *Cryst. Res. Technol.: J. Exp. Ind. Crystallogr.* 2002;37(4):329–39.
- [29] Atkins P, DePaula J. *Physical chemistry*. New York: W. H. Freeman and Company; 2006.
- [30] Sujatha C, Rao GM, Uthanna S. Characteristics of indium tin oxide films deposited by bias magnetron sputtering. *Mater. Sci. Eng.: B* 2002;94(1):106–10.
- [31] Fasaki I, et al. Structural, electrical and mechanical properties of NiO thin films grown by pulsed laser deposition. *Appl. Surface Sci.* 2010;257(2):429–33.
- [32] Reddy YAK, Ajitha B, Reddy PS. Influence of growth temperature on the properties of DC reactive magnetron sputtered NiO thin films. *Int. J. Current Eng. Technol.* 2014;Special issue:351–7.
- [33] Lu Y, Hwang W-S, Yang J. Effects of substrate temperature on the resistivity of non-stoichiometric sputtered NiOx films. *Surface Coatings Technol.* 2002;155(2–3):231–5.
- [34] Chen S, et al. Characterization and properties of NiO films produced by rf magnetron sputtering with oxygen ion source assistance. *Thin Solid Films* 2014;572:51–5.
- [35] Thirumoorthi M, Prakash JTJ. A study of Tin doping effects on physical properties of CdO thin films prepared by sol-gel spin coating method. *J. Asian Ceramic Soc.* 2016;4(1):39–45.
- [36] Madhavi A, et al. Effect of Substrate Temperature on the Structural, Optical and Electrical Properties of Electron Beam Evaporated NiO Thin Films. *Int. J. Adv. Res. Phys. Sci. (IJARPS)* 2014;1:16–20.
- [37] Gibbs ZM, LaLonde A, Snyder GJ. Optical band gap and the Burstein-Moss effect in iodine doped PbTe using diffuse reflectance infrared Fourier transform spectroscopy. *New J. Phys.* 2013;15(7). p. 075020.
- [38] Burstein E. Anomalous optical absorption limit in InSb. *Phys. Rev.* 1954;93(3):632.
- [39] Rahal A, Benramache S, Benhaoua B. Substrate temperature effect on optical property of ZnO thin films. *Eng. J.* 2014;18(2):81–8.
- [40] Bakr N, et al. Refractive index, extinction coefficient and DC conductivity of amorphous arsenic triselenide thin film doped with silver. *Thin Solid Films* 2003;424(2):296–302.
- [41] Bakr NA, Khodair ZT, Hassan SMA. Effect of substrate temperature on structural and optical properties of Cu₂ZnSnS₄ (CZTS) films prepared by chemical spray pyrolysis method. *Research Journal of Chemical Sciences* 2014. ISSN 2231: p. 606X.